European Journal of Computational Mechanics, 2013
Vol. 22, Nos. 2–4, 170–182, http://dx.doi.org/10.1080/17797179.2013.820902

Taylor & Francis
Taylor & Francis Group

Advanced finite element modelling for the prediction of 3D breast deformation

Guillaume Dufaye[a,b], Abel Cherouat[b]*, Jean-Marie Bachmann[a] and Houman Borouchaki[b]

[a]*IFTH Troyes 270 Faubourg Croncels, Troyes 10000, France;* [b]*Gamma3-INRIA Team, Charles Delaunay Institute, University of Technology of Troyes, 12 rue Marie Curie – BP2060 Troyes 10010, France*

The paper aims to study the behaviour of female busts when static or dynamic and must take into account the different biological components of the breast. The numerical simulation of the breast deformability enables the development of new techniques for corsetry or new medical equipment, especially for the detection of breast cancer. In this study, a hyperelastic model of the static behaviour of the bust based on an experimentally-finite element simulation that takes into account the components (skin, fat, glands or fibres and suspensory ligaments of Cooper) responsible for the actual breast deformability under the influence severity is given.

Keywords: breast; reconstitution; modelling; simulation; comsol-multiphysic

1. Introduction

The purpose of this research focuses on the study of the morphology of the female bust during the physical activity to improve the comfort and aesthetics of bras. From the health point of view, it is to develop effective retention (the statistics indicate that 80% of women wear a bra that is unsuitable) and improve the psychological rehabilitation of the convalescent phase of final oncological surgery. Breast imaging is essential for screening, diagnosis of lesions and for early 3D shape reconstitution. Several imaging modalities are used in clinical settings and the breast orientation and positioning procedures differ between the various modalities. X-ray mammography involves compressing the breast between two parallel plates and collecting 2D images at two different acquisition angles and magnetic resonance imaging (MRI), where the patient lies prone with her breasts extending into a specifically designed coil. The shape of the breasts is, therefore, dictated by the gravity load and by any contact between the breast and the coil (Edsander-Nord, Wickman, & Jurell, 1996; Garson et al., 2005; Lorentzen & Lawson, 1987; Page & Steele, 1999; Sinna et al., 2009).

The deformations of breast involving imaging have been previously investigated numerically using finite element analysis. Modelling breast deformations is a challenging problem due to the anatomical complexity of constituents (Figure 1) and uncertainties regarding reliability of biomechanical breast models. Several studies have

*Corresponding author. Email: abel.cherouat@utt.fr

reported the development of breast models with simplifications such as a homogeneous interior (Lorentzen & Lawson, 1987; Page & Steele, 1999), while relatively few report models that include the details of the breast interior. Azar, Metaxas, and Schnall (2002) built a realistic breast model from MR data to track lesions during biopsy. The MR scan was segmented semi-manually and included fibro-glandular tissues, adipose tissues and a lesion. The mechanical properties of the tissues were formulated as non-linear stress–strain curves. More recently, Pathmanathan, Gavaghan, Whiteley, Chapman, and Brady (2008) developed a comprehensive finite element model including the major breast tissue categories and realistic geometry generated from medical images (Catanuto et al., 2008; Kovacs et al., 2007; Lee, Hong, & Kim, 2004; Seo, Cordier, & Hong, 2007).

In this study, we present a virtual deformable breast model of a representative volunteer whose geometry is constructed from MR data. The elastic properties of the deformable model are based on the use of finite elements with non-linear material properties capable of modelling the deformation of the breast under external loading at static and dynamic conditions. All constituents are considered as quasi-incompressible isotropic hyperelastic homogenous (Azar et al., 2002; Del Palomar, Calvo, Herrero, Lopez, & Doblaré, 2008; Gefen & Dilmoney, 2007; Pathmanathan et al., 2008; Roose, De Maerteleire, Mollemans, & Suetens, 2005; Vandeweyer & Hertens, 2002). The proposed numerical modelling is based on the hyperelastic model of the bust based on an experimentally finite element simulation that takes into account the constituents (skin, fat, glands or fibres and suspensory ligaments of Cooper) responsible for the deformability of inhomogeneous soft breast tissues under the effect of gravity.

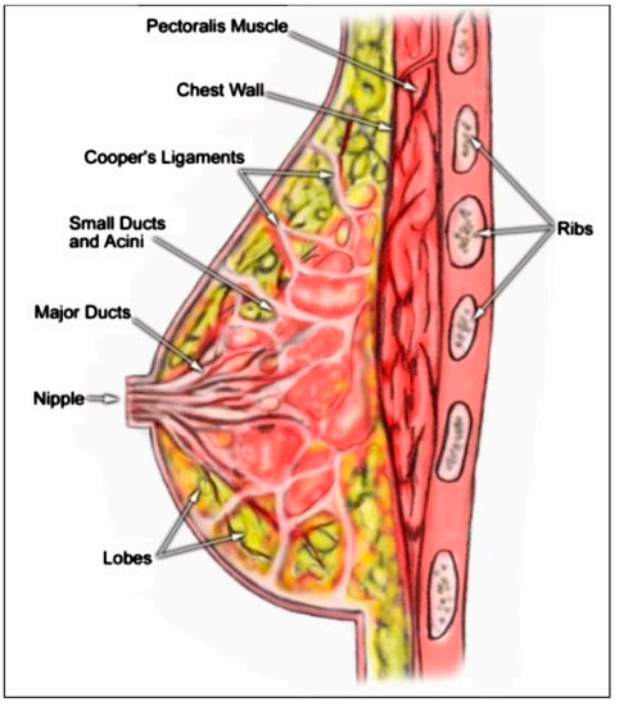

Figure 1. Cup section of the breast (Lorentzen & Lawson, 1987).

2. Reconstitution of the breast

Azar et al. (2002) and Del Palomar et al. (2008) have recently proposed numerical models of breasts using different approaches in order to take into account the internal components of the breast. However, the geometric boundary conditions are different because it is difficult to set a limit. MRI has been set for maximum quality and resolution with a space between sections of 2 mm. Even if the camera moves down to a lower resolution, the image quality is reduced due to volunteers' respiratory movements. MRI is a qualitative review, the optimum setting was chosen after extensive testing, but does not precisely show the Cooper's ligaments. In fact, they do not appear on all cuts and cannot be reconstructed in 3D. Because MRI is a qualitative examination, there is no correspondence between grayscale and materials observed as the ReTomography, and imaging Fat Sat settings were used to highlight different constituents. These settings allow you to observe the skin and its thickness, which is an important consideration for the influence of the skin on the breast behaviour. Segmentation, therefore, cannot be automated and optimised with algorithms known as Otsu and must be done frame by frame manually. This method, although long, provides a good continuity of the components that it is desired to reconstruct with a geometrical error of the order of 2mm. The model was then reconstituted using the Mimics software, removing less than 2 mm that may resemble artefacts due to our segmentation method spaces (Figure 2).

In this study, we have developed a numerical model based on full readings of MRI, where the tissue fibro-glandular appears very clearly in a volume of fat, which allows reconstruction, and inhomogeneous states that with a scanner (Figure 2). The skin is represented by the envelope with a thickness corresponding to the geometric that is applied. The 3D numerical model is based on a reconstruction of MRI images obtained by making a clinical study of 10 healthy volunteers, aged between 19 and 26 years and a medium BMI (between 18 and 25). All volunteers must also have a chest with a C cup minimum to minimise the deformation error that we could observe.

Azar et al. (2002), Del Palomar et al. (2008), Gefen and Dilmoney (2007) have proposed numerical models of breasts using different approaches but with a common goal: to take into account the internal components of the breast. However, the geometric boundary conditions are different, because it is difficult to establish the boundaries of the constituents in the breast, since in our model we have chosen not to take into account geometrical bodies lying behind the breast and limit it to the plane of plexus. This also reduces the factors inaccuracies model since the elastic modulus of the

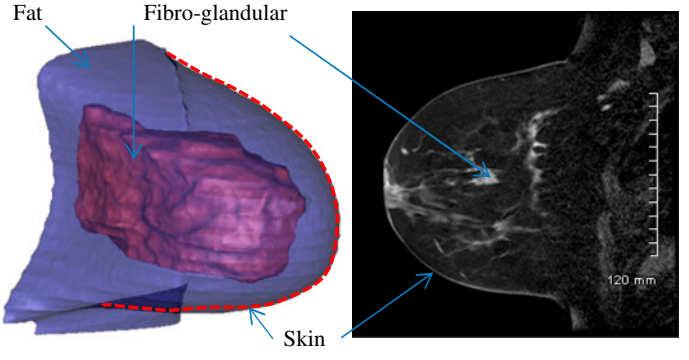

Figure 2. Geometry of the breast and CAD reconstitution with the constituents: skin, fat and fibro-glandular.

pectoral muscle varies greatly from one person to another and from one position to another (Kovacs et al., 2007). The reconstituted geometry of the 3D breast is then meshed using adaptive surface mesher DECIMESH and volumic adaptive mesher OPTIFORM. Given this data, the 3D mesh of the model is generated automatically, and every element in the mesh is assigned a particular tissue type value. 120,563 linear tetrahedral finite elements are used to study the deformability of the breast subjected to gravity (see Figure 3). The contact between skin, fat and glandular tissues is considered as sticky (no slip and no separation).

3. Finite element model

COMSOL is a powerful finite element solver that exploits the benefits of the weak form formulation of partial differential equation problems with Neumann, Dirichlet and Robin (mixed) boundary conditions:

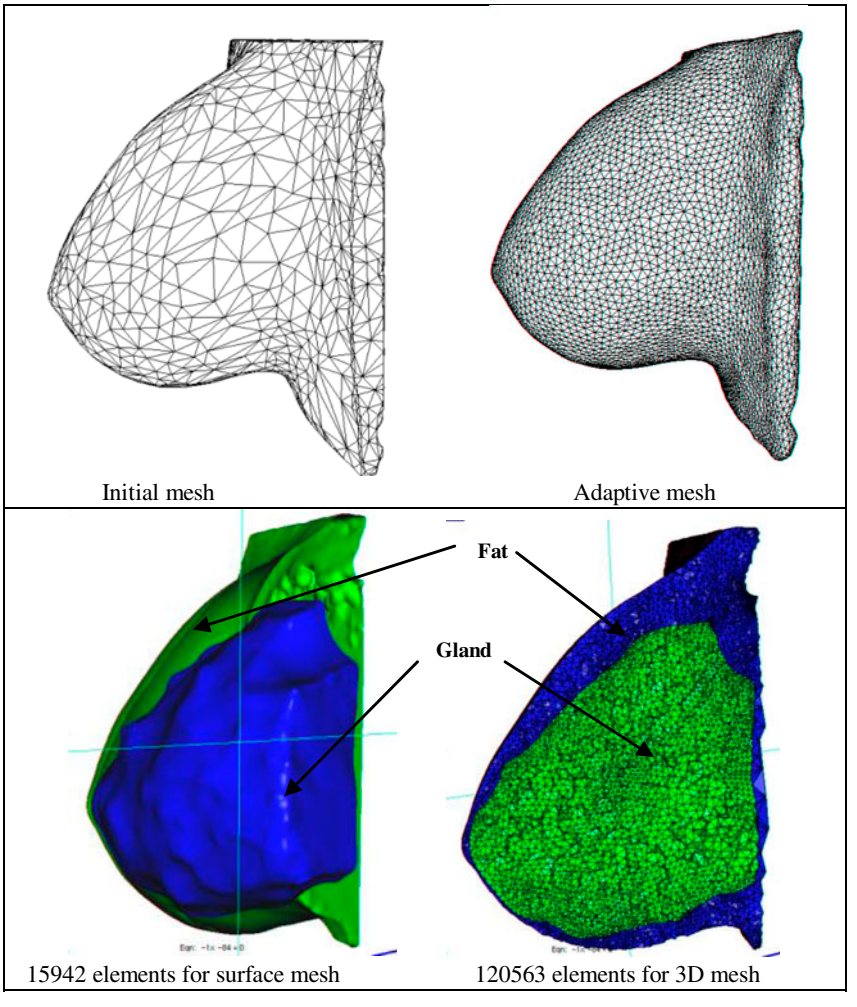

Figure 3. 3D surface and volume mesh of a scanned breast MRI.

$$P = \int_{\Omega_t} (-\underline{\sigma}(u).\nabla u + \vec{\mathbf{f}}.u)d\Omega + \int_{\Gamma_t} \vec{\mathbf{t}}(\mathbf{u}) \cdot \mathbf{u}d\Gamma \tag{1}$$

where $\underline{\sigma}(u)$ is the stress tensor, $(\vec{\mathbf{f}}, \vec{\mathbf{t}})$ are bulk load and boundary loads. The Cauchy stress depends on the displacement (u) through a constitutive equation. The Equation (1) defines a highly non-linear (large deformation large displacements, large rotations) system to express the dynamical equilibrium of the material point. The spatial discretisation and system linearisation are two necessary works to solve this non-linear equation. In this section, it briefly describes a displacement-based finite element method for small strain problems. Most of the basic finite element matrices and arrays are introduced here. At this stage, the underlying material is assumed elastic, so that no time discretisation of the constitutive equations is required and attention can be focused on the finite element discretisation alone.

Using the finite element method, the domains Ω can be divided into sub-domain Ω_e with different element V_e. These elements are considered as iso parametric, which means that the same set of shape functions is used to represent both the element geometry and displacement interpolations. Using classical interpolation of geometry and displacement, the equilibrium Equation (1) for each element is written as follows:

$$I_e(u_e^N, \delta u_e^N) = (\mathbf{M}_e \ddot{u}_e^N + F_e^{int} - F_e^{ext})\delta \dot{u}_e^N \tag{2}$$

where $\mathbf{M}_e$ is the mass matrix associate with element, F_e^{ext} is the vector of external force of element and F_e^{int} is the vector of internal force:

$$\begin{cases} \mathbf{M_e} = \int_{V_e} \rho(\mathbf{N}_N)^T \cdot \mathbf{N_N} dV_e \\ F_e^{ext} = \int_{V_e} \mathbf{N_N} \cdot \vec{\mathbf{f}} dV_e + \int_{\Gamma_e^F} \mathbf{N}_N \cdot \vec{\mathbf{t}} d\Gamma + \int_{\Gamma_e^c} \mathbf{N_N} \cdot \vec{\mathbf{t}}_c d\Gamma \\ F_e^{int} = \int_{V_e} \mathbf{B}_e^{\mathbf{N}} : \sigma dV_e \quad \mathbf{B_e^N} = \frac{\partial \mathbf{N}}{\partial x_N} \end{cases} \tag{3}$$

Note that the $\mathbf{B}_e^{\mathbf{N}}$ is the matrix of the deformation gradient and δu is the global virtual displacement vector and kinematical compatible in the whole structure There are two aspects to be considered to solve the algebraic system above. The first one is solving it in static case, which neglects the inertial effects. The classic or modified Newton–Raphson algorithm is particularly useful in the solution of this non-linear incremental equation. Due to its quadratic rates of asymptotic convergence, this method tends to produce relatively robust and efficient incremental non-linear finite element schemes.

Mechanically, the Cooper's ligaments have an impact on the shape and the mechanical behaviour of the breast in the standing position, when the ligaments are activated (Gefen & Dilmoney, 2007; Simonetti, Huang, Duric, & Littrup, 2009). Therefore, the ligaments can be considered as not activated for the imaging scenarios of interest in this study. Furthermore, their structure is difficult to observe even with advanced scanning techniques such as ultrasound tomography. Other small-scale structures such as blood vessels and milk ducts are not relevant in terms of their contribution to the overall mechanical properties (Gefen & Dilmoney, 2007) and thus will not be included in the model. All tissues are considered as homogenous and quasi-incompressible. Fat, skin and glandular tissues are modelled as non-fibrous gel-like materials, so their mechanical response is considered as isotropic. Furthermore, measurements from Wellman (Wellman & Tactile imaging, 1999) show that the behaviour of these tissues is virtually

linear. Fat tissue, glandular tissue and skin are considered to be quasi-incompressible isotropic hyperelastic material, in the classical Lagrangian formulation. The strain energy potential function of the Neo-Hookean model is expressed in the form:

$$W(\bar{I}_1, D_1) = C_{10}(\bar{I}_1 - 3) + \frac{1}{D_1}(J^{el} - 1)^2 \tag{4}$$

where W is the strain energy per unit of reference volume; $\bar{I}_1 = Tr(\varepsilon)/J^{el}$ is the first deviatoric strain invariant, $J^{el} = \det F$ the elastic volume ratio and C_{10} and D_1 are parameters defining the shear behaviour and the bulk behaviour of each components function of the elastic modulus E and the Poisson's ratio v.

$$C_{10} = \frac{E}{4(1+v)} \quad D_1 = \frac{6(1-2v)}{E} \tag{5}$$

For a compressible material, the Cauchy stress is given by:

$$J^{el}\underline{\sigma} = -pI + \frac{2 \cdot C_{10}}{(J^{el})^{2/3}} \operatorname{dev}(FF^T) \quad p = -\frac{2}{D_1}J^{el}(J^{el} - 1) \tag{6}$$

where F is the deformation gradient tensor. For an incompressible neo-Hookean material with $J^{el} = 1$.

4. Results

To validate the numerical model, the results were compared with experimental results. The following sections present the differences between the experimental measurements and the simulation, as well as effects of some constituent behaviour (fat, gland and skin tissues).

4.1. Effect of the breast morphological hypotheses

Few studies have been made on determining the mechanical properties of tissue in the breast; however, average values of Young's modulus have been calculated for fat, glandular tissue and skin. We test the hypotheses by modifying the material properties of each tissue, such that the stiffness of breast is dominated by the fat tissue or by the glandular tissue or both fat and gland. The material characteristics of each constituent are obtained in the literature (Gefen & Dilmoney, 2007) without considering the skin at first (Table 1). The hypotheses takes into account the influence of different components within the deformed breast, but also stresses observed.

The first case concerns the study of the breast deformation due to gravity considering the mechanical properties of the breast composed only of fat with $E_F = 500$ Pa. In the second case the breast is composed only of gland and the last case, we assume that the reconstructed breast is composed of fat and gland. We used a value of .49 for Poisson's ratio. Figure 4 shows the predicted deformed breast. If we compare the obtained predicted values of the nipple displacement and the experimental values in three cases (see Table 1) we note that only taking account of all components (fat and glands) gives the best results.

Table 1. Maxi displacement function of breast morphological hypotheses.

Morphological hypothesis breast	E_F (Pa)	E_G (Pa)	Maxi predicted displacement (mm)
Fully fat	500	0	157.21
Fully glandular	0	5000	15.72
Fat + gland	500	5000	42.5
Experimental result	39.0 mm		

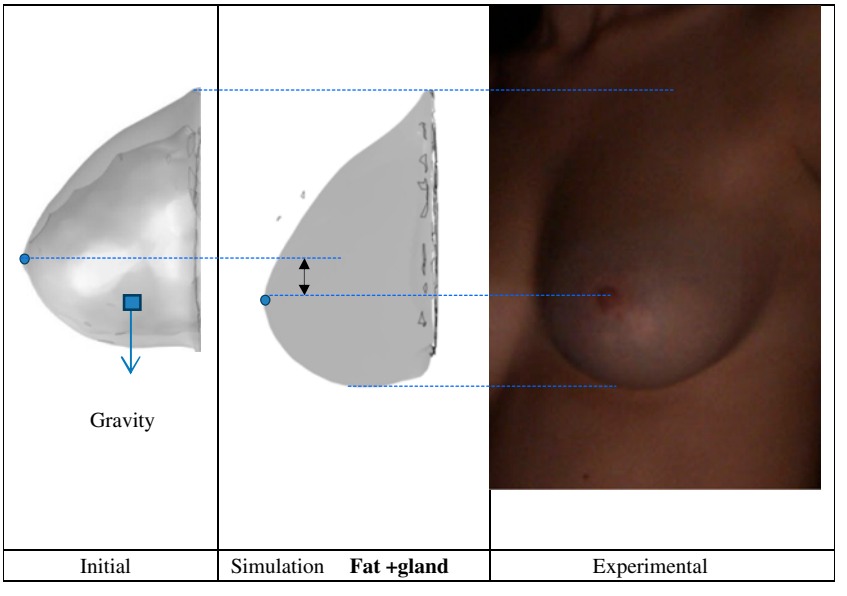

Figure 4. Deformed breast function morphological hypotheses.

4.2. *Effect of the skin behaviour*

It should be noted that Section 4.1, taking into account only the fat and the gland tissues, is highly incomplete. If the influence of Cooper's ligaments on the shape of the breast is still difficult to assess, the influence of the skin is important. According to that, the elastic moduli of the skin of the breasts vary greatly (Gefen & Dilmoney, 2007), so in this section we quantified the influence of the skin modulus ranging from $E_S = 10^3$–10^6 Pa on the breast displacement subject to gravity (Table 2). As Cooper's ligaments are binding on all skin/fat/glands/pectoral muscle in a rigid cohesion, we have chosen to consider no slip and no separation between components. In Figure 5, we show that the maximum displacement of the breast (located at the nipple) ranges from 39.2 mm, when the modulus of the skin E_S is 10^3 Pa. If the skin modulus value then increases the displacement of nipple under gravity is lower. The wide ranges of values of the skin due to the fact that the precise thickness of the breast is not considered. We also note in Figure 5 that the higher the modulus of the skin increases, the lower the deformation of the breast is. This means that it is the behaviour of the skin that keeps the breasts in a given configuration.

Table 2. Displacement and von-Mises stress for different Young's modulus E_S.

E_S (Pa)	1000	10,000	100,000
Displacement (mm)	**39.2**	**26.1**	**9.4**
Maxi Stress in gland (Pa)	12,223	9013	4349
Maxi Stress in skin (Pa)	1642	11,004	90,017

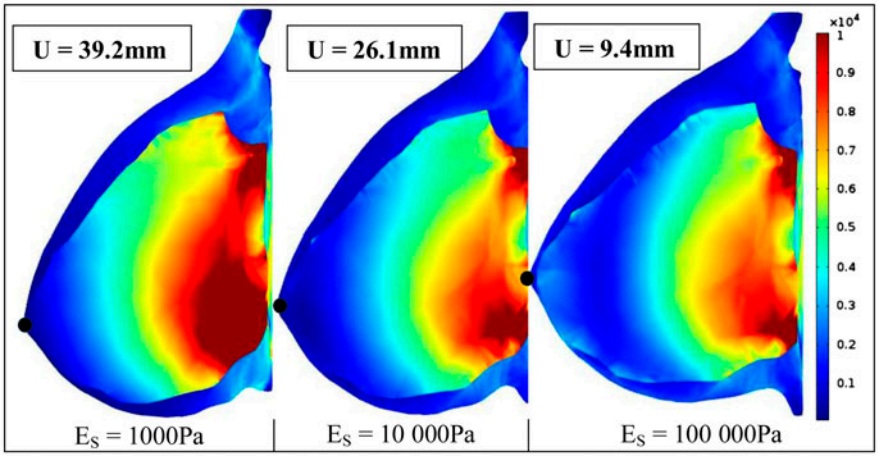

Figure 5. von-Mises stress according to different Young's moduli of the skin.

4.3. *Effect of the skin thickness*

If the Young's modulus E_S has a strong impact on breast behaviour, it would be interesting to study the effect of the skin thickness on the breast deformation. Reconstruction MRI provides a skin model, where the thickness can be accurately measured (Figure 6). Some MRI settings indeed appeared very clearly so that the skin can then be segmented and reconstructed in the same way as fat and gland. Our reference model, we observed a thickness of 1.5 mm in the lateral areas and least variation constraints within 3.5 mm in the weight of the subject areas within. The average thickness observed on the sagittal plane of the breast is 2.5 mm, a value that we have applied to shell elements, shifted out of 1.5 mm. Noting that the consideration of the real thickness of the skin enhances the predicted results, the influence of the thickness of the skin on the breast deformation observed in Table 3 shows that an error of 1 mm in thickness causes changes of more than 25%. The obtained predicted results show that the greater the thickness of the skin increase, the less important the deformation and stress in the fat and glands is. Moreover, it is interesting to note that using embedding or symmetry boundary conditions as breast simulating does not give the same displacement as the bust.

4.4. *Effect of the Poisson's coefficient*

Biomaterials breasts are considered incompressible or almost incompressible. For this, it is common to consider a Poisson coefficient close to 0.5 represents the incompressibility, but it is also possible to use the quasi-incompressible formulation of the equation of second stress tensor of Cauchy stress. The influence of the Poisson coefficient on the

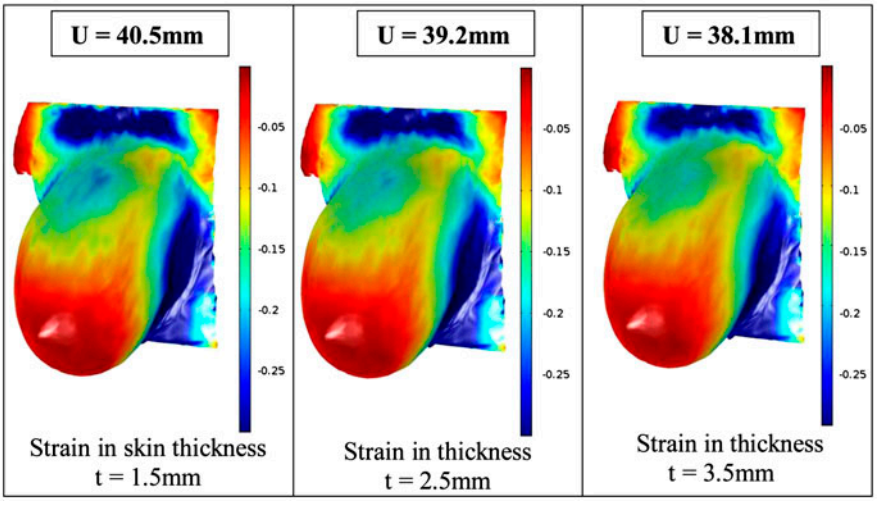

Figure 6. Thickness strain distribution in the skin.

Table 3. Displacement and von-Mises stress depending on the thickness of the skin for $E_F = 500$ Pa, $E_G = 5000$ Pa, $E_S = 1000$ Pa.

Skin thickness (mm)	1.5	2.5	3.5
Displacement (mm)	**40.5**	**39.2**	**38.1**
Maxi Stress in gland (Pa)	12,557	12,223	11,912
Maxi Stress in skin (Pa)	1655	1642	9226

breast deformation observed in Table 4 shows that an error of .1 in Poisson coefficient causes small changes in the breast deformation. Noting that, considering more components are quasi-incompressible over the predicted results are improved. The obtained numerical results confirm that the components of the breast are almost incompressible.

5. Inverse approach

To obtain the elastic parameters of the breast constituents an inverse numerical-experimental approach is used. The inputting data are obtained with ten women volunteers in order to achieve an average model, which is representative of a large group of people. To study the effect of breast deformability under the effect of gravity at different positions the suprasternal notch taking as a fixed reference is used in order to obtain the nipple displacements along the two plane axes (Figure 7).

Table 4. Effect of Poisson modulus on the maximum displacement of breast.

Poisson coefficient	$\nu = 0.4$	$\nu = 0.49$	(Incompressible) $\nu = 0.5$
Maxi displacement (mm)	**44.5**	**39.2**	**38.8**
Maxi Stress in gland (Pa)	21,501	12,223	12,712
Maxi Stress in skin (Pa)	1769	1642	1721
CPU time (s)	41	66	84

To determine the hyperelastic parameters of breast (fat, glands and skin), the algorithm implemented in Comsol was used. This algorithm changes asset of hyperelastic parameters systematically to find the parameter set that yields the best FE displacement fit to its measured response.

For each applied load gravity iteration, the equation of motion must be solved and the intermediate model node displacements of nipple (reference point) are calculated. Following that step, the elasticity value of every element in the model is updated given its load value and the linear material model of the tissue type it represents. This optimisation process is iterative, with the first step being the construction of the tissue specimen's FE mesh. Next, the hyperelastic parameters are initialized to create the FE Neo-Hookean hyperelastic model, followed by inputting the nipple displacements data and starting FE analysis. In this study, the Nelder – Mead algorithm has been tested to more reliable results. In all simulations, the iterative process was terminated when the specified tolerance condition was met, at a maximum of 1000 iterations, or when the least-squares error measure displayed no improvement. To ensure uniqueness of the calculated parameters, the optimisation algorithm was performed with various initial estimates. It was found that the final calculated parameters for every model were independent of the initial estimates. The simplex optimization algorithm was used to minimise the R^2 average (Nelder & Mead, 1965) value by generating new parameter sets for the FEMs. This optimisation algorithm was chosen because it is simple and converged quickly for this problem.

The elastic modulus was optimised for all tissue by minimising the mean squared error (MSE) between the simulated and experimental displacement curves using the nonlinear minimisation routine available in Comsol. MSE is defined as follows:

$$\mathrm{MSE} = (|u_{\mathrm{model}}| - |u_{\mathrm{exp}}|) \tag{7}$$

The restitution of the geometry of real deformable breast of representative volunteers under the gravity effect from Inspeck tool reconstitution data is given in Figure 7. A study of the effect of morphological constituents of the numerical model taking into account fat, gland and skin was performed. Three cases are proposed to investigate the influence of the properties of each component on the deformation of the breast. In the first and second case, considering that the properties of skin are predominate (ranging from 15,000 to 50000Pa) compared to the properties of glands and fat. In the first case

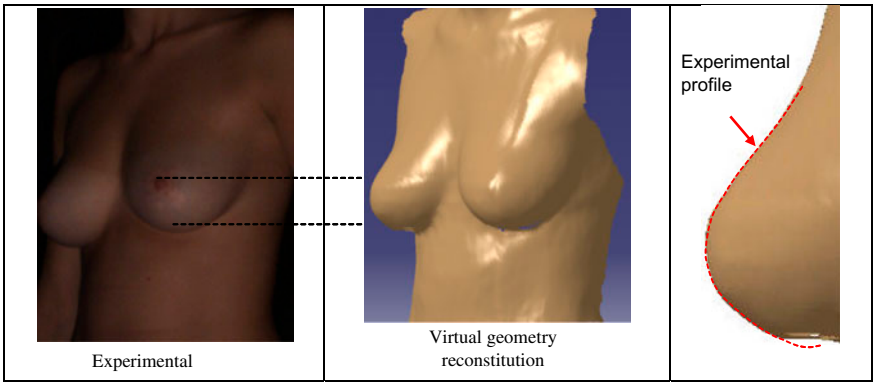

Figure 7. Experimental result and deformable breast profile reconstitution.

the glands and fat modules are more important than in the second case. In the latter case, an optimization procedure is used to find the best values of the components responsible for the deformation of the breast. Values obtained from the optimization inverse approach are given in Table 5.

The predicted profile of the deformed breast under gravity is compared with the experimental one in Figure 8. The FE analysis indicated that the maximum displacement reaches as much as 39.4 mm in the region underneath the nipple. We note that the maximum value is about 1000 Pa and reached in the gland component. The effect of E on displacement of nipple error was small (0.2 mm average $\leqslant$ 1 mm maximum). The results of the profiles of breasts deformed by gravity with the inverse approach are in good agreement with the experimental profiles of the experiment in comparison with the other two cases where the modules are offered randomly. They show the importance of the inverse optimization which considers only the fat and glands modules which vary separately in the simulations based on the deformation of the breast. We can note that, in case 1, the maximum displacement of the nipple is about 39.4 mm, whereas in case 2, the maximum displacement is about 39.3 mm. The third case has softer fat altogether, but a harder gland collapses in a sliding along the wall pectoral, generating large breast elongations, and therefore major stresses despite large lower displacement, and confirms the strong influence of the skin on the maximum displacement.

Table 5. Nipple displacement according to 3 cases of breast properties.

Case	Elastic properties (Pa)	Displacement of nipple (mm)
Case 1	$E_F = 1000$ $E_G = 1000$ $E_S = 15{,}000$	39.4
Case 2	$E_F = 100$ $E_G = 100$ $E_S = 50{,}000$	39.3
Case 3 Inverse approach	$E_F = 500$ $E_G = 5000$ $E_S = 1000$	39.2

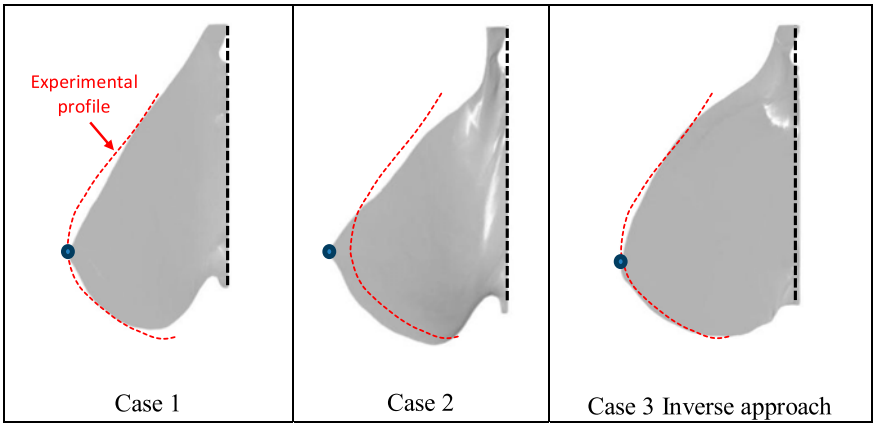

Figure 8. Deformed shapes of breasts for 3 cases.

Table 6. Predicted modulus of breast tissue compared with literature values.

Elastic modulus (kPa)	Roose et al. (2005)	Tanner et al. (2006)	Gefen and Dilmoney (2007)	Our results 2013
Gland tissue	1.7–500	1–20	7.5–66	0.5–10
Fat tissue	1.7–500	1	0.5–25	0.1–2
Skin			200–3000	10–300

The maximum principal strain in the deformed configuration, reaches values up to about 80%. There is good agreement between the two results, thus showing the efficiency of the proposed inverse approach. In Table 6, we compare the optimised elastic modulus of breast components with the literature values. We note that the intervals of the obtained modulus of breast tissue are smaller than those of the literature.

6. Conclusion

This study concerns the restitution of the geometry of virtual deformable breast of representative volunteers from MR clinical data. What is well argued is that the mechanical properties of the breast skin play an important role in explaining the changes associated with radiotherapy, tissue expansion, and breast reconstruction surgery. The proposed numerical modelling takes into account the main constituents such as skin, fat, glands or fibres and suspensory ligaments of Cooper, responsible for the deformability of breast tissues under the effect of gravity. The final results show that it is possible to create a deformable model of the breast based on the use of finite elements with linear material properties capable of modelling and predicting the deformation of the breast. The 3D reconstruction and numerical calculations using a finite element method including the inverse optimisation approach showed the effectiveness of the proposed approach. This numerical methodology can be used as a tool for future work and concerns the establishment of a reliable simulation method that could help the development of new techniques for bras, corsetry or new medical equipment, especially for the detection of breast cancer.

Acknowledgements

The financial support of the FEDER and CRCA for the regional BRAMMS project D201003616 is gratefully acknowledged.

References

Azar, F. S., Metaxas, D. N., & Schnall, M. D. (2002). Methods for modelling and predicting mechanical deformations of the breast under external perturbations. *Medical Image Analysis, 6*, 1–27.

Catanuto, G., Spano, A., Pennati, A., Riggio, E., Farinella, G. M., Impoco, G., … Nava, M. B. (2008). Experimental methodology for digital breast shape analysis and objective surgical outcome evaluation. *Journal of Plastic Reconstructive and Aesthetic Surgery, 61*, 314–318.

Del Palomar, A. P., Calvo, B., Herrero, J., Lopez, J., & Doblaré, M. (2008). A finite element model to accurately predict real deformations of the breast. *Medical Engineering & Physics, 30*, 1089–1097.

Edsander-Nord, A., Wickman, M., & Jurell, G. (1996). Measurement of breast volume with thermoplastic casts. Scandinavian *Journal of Plastic and Reconstructive Surgery and Hand Surgery, 30*, 129–132.

Garson, S., Delay, E., Sinna, R., Delaporte, T., Robbe, M., & Carton, S. (2005). 3D evaluation and mammary augmentation surgery. *Annales de chirurgie plastique esthétique, 50*, 643–651.

Gefen, A., & Dilmoney, B. (2007). Mechanics of the normal female breast. *Technology and Health Care*, *15*, 259–271. IOS Press.

Kovacs, L., Eder, M., Hollweck, R., Zimmermann, A., Settles, M., Schneider, A., … Biemer, E. (2007). Comparison between breast volume measurement using 3D surface imaging and classical techniques. *The Breast*, 16, 137–145.

Lee, H. Y., Hong, K., & Kim, E. A. (2004). Measurement protocol of women's nude breasts using a 3D scanning technique. *Applied Ergonomics, 35*, 353–359.

Lorentzen, D., & Lawson, L. (1987). Selected sports bras: A biomechanical analysis of breast motion while jogging. *The Physician and Sports Medicine, 15*, 128–139.

Nelder, J., & Mead, R. (1965). A simplex method for function minimization. *Computer Journal, 7*, 308–313.

Page, K. A., & Steele, J. R. (1999). Breast motion and sports brassiere design: Implications for future research. *Sports Medicine, 27*, 205–211.

Pathmanathan, P., Gavaghan, D. J., Whiteley, J. P., Chapman, S. J., & Brady, J. M. (2008). Predicting tumor location by modeling the deformation of the breast. *IEEE Transactions on Biomedical Engineering, 55*, 2471–2479.

Wellman, P. S. (1999). *Tactile imaging*. (PhD thesis). University of Harvard Press, Harvard, IL, USA.

Roose, L., De Maerteleire, W., Mollemans, W., & Suetens, P. (2005). Validation of different soft tissue simulation methods for breast augmentation. *International Congress Series, 1281*, 485–490.

Seo, H., Cordier, F., & Hong, K. (2007). A breast modeler based on analysis of breast scans. *Computer Animation and Virtual Worlds, 18*, 141–151.

Simonetti, F., Huang, L., Duric, N., & Littrup, P. (2009). Diffraction and coherence in breast ultrasound tomography: a study with a toroidal array. *Medical Physics, 36*, 2955–2965.

Sinna, R., Garson, S., Taha, F., Benhaim, T., Carton, C., Delay, E., & Robbe, M. (2009). Evaluation of 3D numerisation with structured light projection in breast surgery. *Annales de chirurgie plastique esthétique, 54*, 317–330.

Tanner, C., Schanabel, J. A., Hill, D. L. G., & Hawkes, D. J. (2006). Factors influencing the accuracy of biomechanical breast models. *Medical Physics, 33*, 1758–1769.

Vandeweyer, E., & Hertens, D. (2002). Quantification of glands and fat in breast tissue: An expérimental determination. *Annals of Anatomy, 184*, 181–184.